Available online at www.sciencedirect.com
SCIENCE DIRECT®
ELSEVIER
Nuclear Instruments and Methods in Physics Research A 528 (2004) 71–77
NUCLEAR INSTRUMENTS & METHODS IN PHYSICS RESEARCH Section A
www.elsevier.com/locate/nima

Overview of the 100 mA average-current RF photoinjector

D.C. Nguyen[a,*], P.L. Colestock[a], S.S. Kurennoy[a], D.E. Rees[a], A.H. Regan[a], S. Russell[a], D.L. Schrage[a], R.L. Wood[a], L.M. Young[a], T. Schultheiss[b], V. Christina[b], M. Cole[b], J. Rathke[b], J. Shaw[c], C. Eddy[c], R. Holm[c], R. Henry[c], J. Yater[c]

[a] *Los Alamos National Laboratory, MS H851, Los Alamos, NM 87545, USA*
[b] *Advanced Energy Systems, Medford, NY 11763, USA*
[c] *Naval Research Laboratory, Washington, DC 11763, USA*

Abstract

High-average-power FELs require high-current, low-emittance and low-energy-spread electron beams. These qualities have been achieved with RF photoinjectors operating at low-duty factors. To date, a high-average-current RF photoinjector operating continuously at 100% duty factor is yet to be demonstrated. The principal challenges of a high-duty-factor normal-conducting RF photoinjector are related to applying a high accelerating gradient continuously, thus generating large ohmic losses in the cavity walls, cooling the injector cavity walls and the high-power RF couplers, and finding a photocathode with reasonable Q.E. that can survive the poor vacuum of the RF photoinjector. We present the preliminary design of a normal-conducting 700 MHz photoinjector with solenoid magnetic fields for emittance compensation. The photoinjector is designed to produce 2.7 MeV electron beams at 3 nC bunch charge and 35 MHz repetition rate (100 mA average current). The photoinjector consists of a $2\frac{1}{2}$-cell, π-mode, RF cavity with on-axis electric coupling, and a non-resonant vacuum plenum. Heat removal in the resonant cells is achieved via dense arrays of internal cooling passages capable of handling high-velocity water flows. Megawatt RF power is coupled into the injector through two tapered ridge-loaded waveguides. PARMELA simulations show that the $2\frac{1}{2}$-cell injector can produce a 7 μm emittance directly. Transverse plasma oscillations necessitate additional acceleration and a second solenoid to realign the phase space envelopes of different axial slices at higher energy, resulting in a normalized rms emittance of 6.5 μm and 34 keV rms energy spread. We are developing a novel cesiated p-type GaN photocathode with 7% quantum efficiency at 350 nm and a cesium dispenser to replenish the cathode with cesium through a porous silicon carbide substrate. These performance parameters will be necessary for the design of the 100 kW FEL.

PACS: 41.60.Cr; 29.17.+w; 29.27.Bd; 41.75.Fr

Keywords: FEL; Photoinjector; High current; High brightness; cw; Photocathode

*Corresponding author. Tel.: +1-505-667-9385; fax: +1-505-667-8207.
E-mail address: dcnguyen@lanl.gov (D.C. Nguyen).

0168-9002/$ - see front matter © 2004 Published by Elsevier B.V.
doi:10.1016/j.nima.2004.04.021

1. Introduction

High-brightness electron photoinjectors (PI) have long been recognized as the enabling technology for short-wavelength vacuum ultraviolet and X-ray FEL, the so-called fourth-generation light sources [1]. PI are also the key component for high-power, high-duty-factor FEL at longer wavelengths, as the high-current, low-emittance and low-energy-spread electron beams lead to high gain, efficient and robust lasing, and reduce unwanted stray particles that can impact or even preclude high-duty operation.

State-of-the-art high-average-current PI come in three different designs: DC PI consisting of a DC electron gun followed by superconducting RF linac, superconducting RF PI with niobium cavities, and normal conducting RF PI with copper cavities. An example of the DC PI is the Jefferson Laboratory DC gun [2] which is the only true cw photoinjector. This DC PI has produced bunch charges of about 0.14 nC using a GaAs photocathode and a green drive laser. At a repetition rate of 75 MHz the DC PI produces an average current of 10 mA and normalized emittance of 7.5 μm. The superconducting RF PI is under development at FZ Rossendorf [3]. So far the SRF PI has produced low bunch charges.

The normal conducting RF PI, first invented at Los Alamos [4], is now employed in several FEL around the world. These PI typically operate at low-duty factor, very high gradients (20–100 MV/m) and nanocoulomb bunch charges. None of the normal conducting RF PI has operated at 100% duty factor, defined as the fraction of time RF is applied to the PI structure. The highest average current, 32 mA, has been achieved with the Boeing PI (in collaboration with Los Alamos) at 25% duty factor [5]. It uses a K_2CsSb photocathode and 433 MHz cavities to produce 3 nC, 7 μm beams at 5 MeV. The photocathode lifetime is 2–3 h at this duty.

Our objective is to increase the duty factor of normal conducting RF PI to full cw operation. Operating a normal conducting PI continuously presents three main challenges. First, a high accelerating gradient must be applied at the cathode to control the space charge induced expansion that would lead to space-charge and RF induced emittance growth. Second, the continuously applied RF field generates surface current that causes ohmic losses in the cavity walls. These ohmic losses, which scale with the square of the accelerating gradient, drive the RF power requirement to megawatt klystrons and present significant thermal engineering challenges. Third, with cw operation the vacuum in the PI cavities could degrade to a point where any photocathode with reasonable Q.E. can only survive for a short time as contaminants released by stray energetic electrons strike the cathode and poison it.

To address the above challenges, one must optimize the RF PI operating parameters such as RF frequency, accelerating gradient, photoemission radius, cavity cooling, and vacuum requirements for photocathode Q.E. and lifetime. An optimal design is a trade-off involving beam dynamics requirements, RF power, and feasibility of injector cavity cooling.

We present an overview of the cw normal-conducting 700 MHz PI capable of delivering more than 100 mA average current (e.g. 3 nC per bunch at 35 MHz repetition rate) at 2.7 MeV. The average current is scalable to higher values by increasing the bunch repetition rate. The RF PI is designed to operate at a cw gradient of 7 MV/m. The beam transverse normalized rms emittance is 6.5 μm and rms energy spread is 34 keV. We are considering the use of Cs_2Te, Cs:GaN and K_2CsSb photocathodes that require frequency quadrupled, tripled and doubled Nd drive laser, respectively.

2. Injector design

2.1. Cavity design

The cw RF PI is a $2\frac{1}{2}$-cell, π-mode, oxygen-free copper-on-Glidcop® 700 MHz structure with on-axis electric coupling and emittance compensation [6]. The design is a compromise between maximizing the gradient and minimizing the copper surface heat flux. Details of the cavity design can be found in Ref. [7].

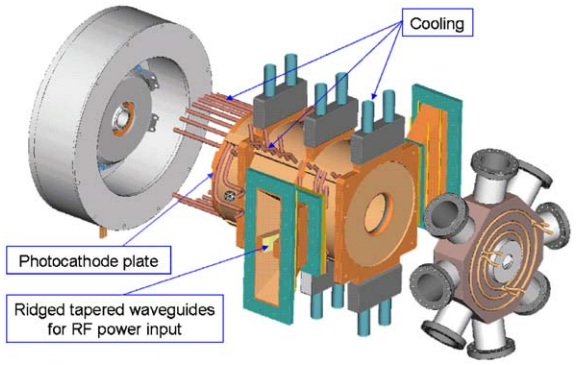

Fig. 1. Schematic of the $2\frac{1}{2}$-cell RF cavity (center) with emittance-compensating magnets (left) and vacuum plenum (right).

The RF PI model, including cooling and RF tapered ridge-loaded waveguides, is shown in Fig. 1. With aperture radius of 65 mm and septum thickness of 20 mm, the cell coupling is 0.03 and the π-mode is well separated from its nearest neighbors. The operating parameters of the cw RF PI are listed in Table 1. The choice of 7 MV/m gradient is dictated by space charge mitigation and cavity thermal management. The on-axis electric field in the π-mode PI has a flat distribution (Fig. 2). The field alternates from one cell to another, and reaches about 10 MV/m near the cathode. RF fields in the vacuum plenum are small since it is resonant at 650 MHz.

Wall power densities are calculated with Superfish and MicroWave Studio. The surface current distribution is shown in Fig. 3. The highest power density is on the cell septa and on the 1st half-cell end wall, where it reaches 105 W/cm^2 at 7 MV/m.

The RF feeds are in the 3rd cell of the $2\frac{1}{2}$-cell PI. Two symmetrically placed ridge-loaded tapered waveguides are connected to the cavity via "dog-bone" coupling irises—long narrow slots with two circular holes at their ends—in a 0.5″-thick copper wall. This design [8] is based on the LEDA RFQ and SNS high-power RF couplers. The required cavity-waveguide coupling is given by the coefficient $\beta_c = (P_w + P_b)/P_w \approx \frac{4}{3}$, where $P_w = 780$ kW is the cw ohmic losses, and $P_b = 270$ kW is the beam power of a 100 mA beam at the injector exit. The coupling is adjusted by changing the radius of the holes at the ends of the coupler slot.

Table 1
Normal-conducting cw RF photoinjector parameters

Bunch charge	3 nC
Accelerating gradient	7 MV/m
Beam energy at injector end	2.7 MeV
Cavity ohmic losses	780–820 kW
Solenoid magnetic field, max	0.37 T
Normalized emittance, rms	7 μm
Bunch length, rms	9 ps
Energy spread, rms	34 keV

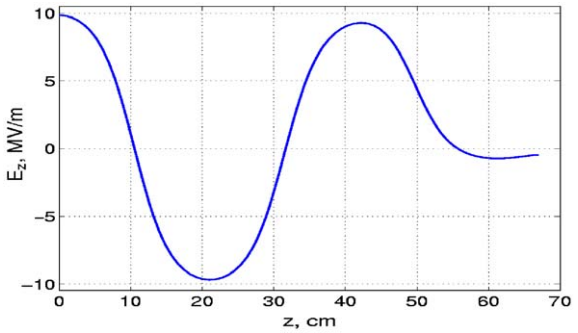

Fig. 2. Electric field distribution in the π-mode of $2\frac{1}{2}$-cell cavity.

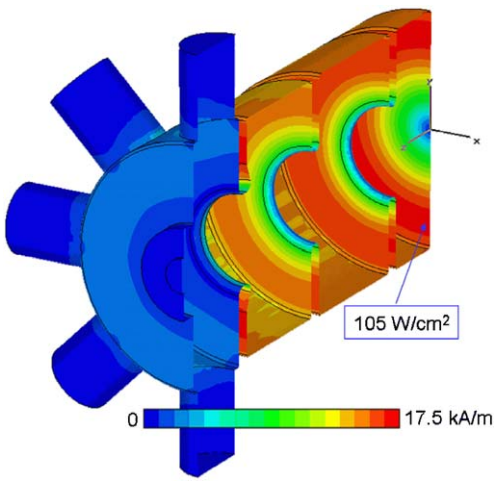

Fig. 3. Surface current distribution in the π-mode of $2\frac{1}{2}$-cell cavity.

2.2. Cathode radius optimization

Space-charge induced emittance scales inversely with the photoemission radius

$$\varepsilon_{n,sc} = \frac{I}{\gamma' I_A\left(3\sigma_r/\sigma_z + 5\right)} \tag{1}$$

where $\gamma' = eE/mc^2$ is the normalized gradient [9]. In the absence of a solenoid, the RF emittance term scales with the square of rms photoemission radius [9]

$$\varepsilon_{\mathrm{n,rf}} = \gamma' k_{\mathrm{rf}}^2 \sigma_z^2 \sigma_r^2. \tag{2}$$

Thermal emittance scales linearly with the photoemission radius

$$\varepsilon_{\mathrm{n,thermal}} = \frac{r}{2}\sqrt{\frac{kT}{mc^2}}. \tag{3}$$

The normalized emittance for a thermalized beam is the quadrature sum of the above three terms.

$$\varepsilon_{\mathrm{n}} = \sqrt{\varepsilon_{\mathrm{n,sc}}^2 + \varepsilon_{\mathrm{n,rf}}^2 + \varepsilon_{\mathrm{n,thermal}}^2}. \tag{4}$$

Without a solenoid field, an optimum cathode radius exists where emittance is minimized. With solenoid magnetic focusing near the cathode, the RF emittance term, caused by transverse RF field at the apertures, is significantly reduced as the beam size decreases at the apertures. Thus, solenoid magnetic focusing leads to a smaller normalized emittance, approaching the thermal emittance limit.

2.3. Beam dynamics simulations

Beam dynamics simulations with PARMELA illustrate the effects of transverse plasma oscillations [10]. For the $2\frac{1}{2}$-cell injector and an initial double Gaussian temporal profile and top-hat spatial distribution, PARMELA output predicts an evolution of emittance that has two minima along the z-axis (Fig. 4). The first minimum occurs when different phase space ellipses line up as a result of the emittance compensation, and the second minimum occurs at a larger emittance when the phase-space ellipses realign. Adding booster linacs to increase the beam energy and a second solenoid to rotate the phase-space ellipses further reduce the normalized rms emittance (Fig. 5). Transverse plasma oscillations cause different phase-space ellipses to rotate and realign at higher beam energy. This results in a

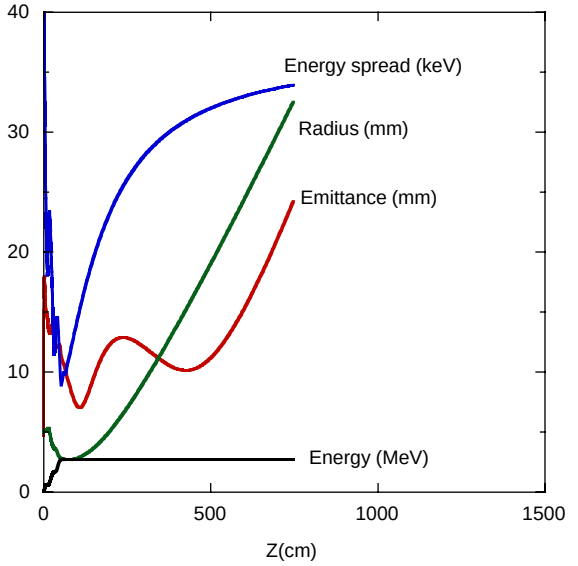

Fig. 4. Calculated normalized emittance, radius, energy and energy spread versus distance ($2\frac{1}{2}$-cell injector with a solenoid magnet).

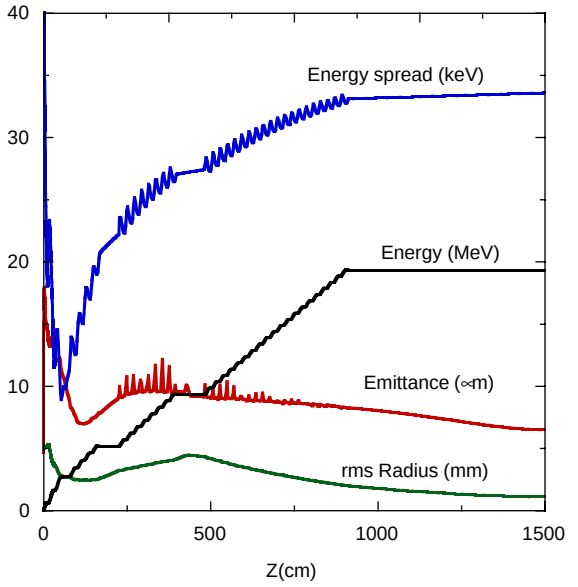

Fig. 5. Calculated normalized emittance, radius, energy and energy spread versus distance ($2\frac{1}{2}$-cell injector with a solenoid plus a 4-cell booster, two additional linacs and a second solenoid).

second minimum further downstream with a lower emittance of 6.5 μm. The rms energy spread is 34 keV. At 19.3 MeV beam energy, the relative energy spread is 0.18%.

3. Thermal management

About 800 kW of RF power is deposited on the walls of the water-cooled PI $2\frac{1}{2}$-cell cavity. This requires a dense array of cooling channels close to the RF surface and a large flow of cooling water for heat removal [11]. Flow requirements based on RF heat loads at surface temperature are reasonable: 36 l/s at 5 m/s with inlet water temperature of 20°C and mean outlet temperature 26°C; see temperature distribution in Fig. 6.

An axisymmetric model of the cavity was developed using the finite element code ANSYS. RF loads were mapped on the surface from SF output and modified based on the surface temperature. Significant stresses generally occur between the heated RF surface and cooling channels. Glidcop® is used throughout this cavity. It has yield strength of 270 MPa and provides significant margin for this design. The resulting steady-state von Mises local stresses do not exceed 68 MPa (Fig. 7). The calculated surface current distribution near the RF coupler irises is shown in Fig. 8. The localized regions of high heat flux will be cooled with dedicated channels in the thick cavity walls.

4. Photocathode development

The choice of photocathode suitable for use in the high-current RF PI is determined by the cathode Q.E., the photon energy needed for photoemission, and the cathode ruggedness toward contamination. We consider three different photocathode materials: Cs_2Te, cesiated p-type GaN, and K_2CsSb. Table 2 summarizes the three photocathodes under consideration for use in the high-current RF PI.

Cesiated p-type GaN is a new photocathode material that has high Q.E. at the third harmonic of Nd lasers. Cesiated GaN is a compromise between the rugged but UV-driven Cs_2Te cathode and the short-lived, green-driven K_2CsSb cathode. We have studied the sensitivity of Cs:GaN to exposure to carbon monoxide. The Q.E. versus wavelength at different CO exposure durations are plotted in Fig. 9.

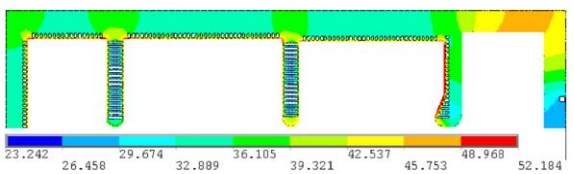

Fig. 6. Temperature distribution of the RF PI with realistic cooling.

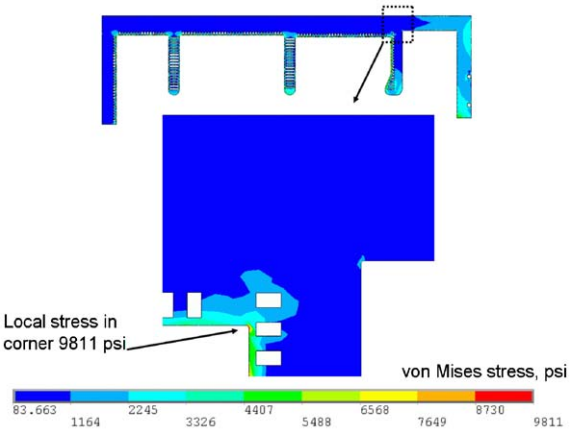

Fig. 7. Stress distribution in the RF photoinjector cavity.

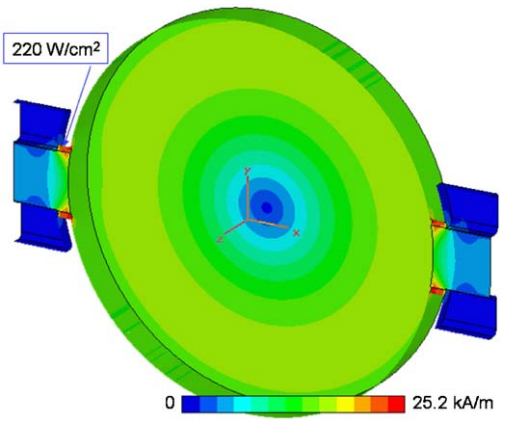

Fig. 8. Surface current distribution near the RF coupler irises.

Table 2
Photocathodes being considered for use in the cw RF photoinjector

	Q.E. (%)	Wavelength (nm)	Lifetime (h)
Cs_2Te	3	263	40
Cs:p-GaN	7	350	20
K_2CsSb	8	530	3

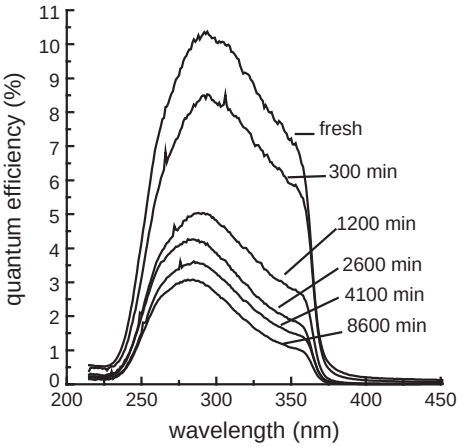

Fig. 9. Cs:GaN response curves at different CO exposure times.

A cathode that responds to lower energy photons is a better choice since it uses less laser power. At the same Q.E., K_2CsSb uses half as much laser power as Cs_2Te. With a 20% green-to-UV conversion efficiency, K_2CsSb uses ten times less IR power than Cs_2Te. Cs_2Te thus requires a larger and more complex drive laser than K_2CsSb.

However, K_2CsSb cathodes lose their Q.E. in the matter of a few hours. Their photoresponse can be rejuvenated with occasional re-cesiation but this process is time consuming and is not conducive to continuous operation. A solution to this problem is to use a cesium dispenser behind the photocathode to continuously replenish it with cesium. To this end, we use semi porous SiC as possible substrates for the above photocathodes. Preliminary studies show that at 400–600°C the released Cs diffuses through SiC and deposits on the surface at a rate of 1–3 Å s^{-1}.

5. Conclusions

We present an overview of the physics design of the 100 mA average-current RF photoinjector. This normal-conducting cw RF photoinjector is a $2\frac{1}{2}$-cell, π-mode, 700 MHz structure made out of oxygen-free copper on Glidcop® with on-axis electric coupling and emittance compensation. At an accelerating gradient of 7 MV/m, the output beam will have 2.7 MeV kinetic energy, 7 μm normalized rms emittance, 9 ps rms bunch length and 34 keV rms energy spread. The total ohmic losses in the injector are about 800 kW, with a maximum heat flux slightly above 100 W/cm^2. Thermal analysis shows that the heat due to ohmic losses can be effectively removed with water cooling through a dense array of cooling channels.

Cooling the regions around the coupling irises is a challenging thermal management issue because the surface heat flux exceeds 200 W/cm^2 at a few hot spots. However, these hot spots are localized around the ends of the dog-bones and can be cooled effectively with cooling channels placed properly around the slots in the thick cavity wall.

We are in the process of finalizing the engineering design and fabricating the cold cavity model. Our plan is to construct the full-power prototype and install it in the Low Energy Demonstration Accelerator facility at LANL to perform RF and thermal tests without beam in late 2004. Once the RF tests and thermal management with high heat flux have been successfully demonstrated, the system will be upgraded to operate at 100 mA average current with the addition of a photocathode, a drive laser, a second klystron, and beam diagnostics.

References

[1] D.C. Nguyen, et al., Phys. Rev. Lett. 81 (1998) 810.
[2] T. Siggins, et al., Nucl. Instr. and Meth. A 475 (2001) 549.
[3] E. Barhels, et al., Nucl. Instr. and Meth. A 445 (2000) 408.
[4] J.S. Fraser, R.L. Sheffield, E.R. Gray, Nucl. Instr. and Meth. A 250 (1986) 71.
[5] D.H. Dowell, et al., Appl. Phys. Lett. 63 (1993) 2035.
[6] B.E. Carlsten, Nucl. Instr. and Meth. A 285 (1989) 313.

[7] S.S. Kurennoy, et al.,'Development of Photoinjector RF Cavity for High Power FEL,' Nucl. Instr. and Meth. A (2003), these Proceedings.
[8] S.S. Kurennoy, L.M. Young, 'RF Coupler for High-Power CW FEL Photoinjector,' Proceedings of the 2003 Particle Accelerator Conference, p. 3515.
[9] K.J. Kim, Nucl. Instr. and Meth A 275 (1989) 201.
[10] L. Serafini, J.B. Rosenzweig, Phys. Rev. E 55 (1997) 7565.
[11] A.M.M. Todd, et al.,'High-power electron beam injectors for 100 kW free-electron lasers,' Proceedings of the 2003 Particle Accelerator Conference, p. 977.